Study of Electron Cloud Effects in the DAΦNE Φ-Factory for the KLOE-2 Run

Theo Demma*

INFN, Laboratori Nazionali di Frascati,

via E. Fermi 40, 00044 Frascati, RM, Italy

Abstract

A strong horizontal instability has been observed in the the DAΦNE positron ring since 2003. Experimental observations suggest an electron cloud induced coupled bunbh instability as a possible explanation. Here is reported a simulation study of the eleatron cloud effefts in the positron ring of the DAΦNE Φ factory with particular reference to the machine configuration designed for the KLOE-2 experiment.

* theo.demma@lnf.infn.it

I. INTRODUCTION

After the 2003 shutdown for the FINUDA detector installation, and some optics and hardware modifications, the appearance of a strong horizontal instability for the positron beam at a current $I_{th.} = 500$ mA, triggered the study of the e-cloud effect in the DAΦNE collider. Experimental observations that seem to provide an evidence that the electron cloud effects are present in the DAΦNE positron ring can be summarized as follow: a larger positive tune shift is induced by the positron beam current [1]; the horizontal instability rise time cannot be explained only by the beam interaction with parasitic HOM or resistive walls and increase with bunch current [2]; the anomalous vacuum pressure rise with beam current in positron ring [3], bunch-by-bunch tune shifts measured along the DAΦNE bunch train present the characteristic shape of the electron cloud build-up [4]. There are also indications that wigglers play an important role in the instability, since the main changes after the 2003 shutdown were the modification of the wiggler poles, and lattice variation which gave rise to an increase of the horizontal beta functions in wigglers [5]. To better understand the electron cloud effects and possibly to find a remedy, a detailed simulation study is undergoing. In this paper we present recent simulation results relative to the build up of the electron cloud in the DAΦNE wiggler and in straight sections in presence of a solenoid magnetic field. Then we estimate the electron cloud induced instabilities in the DAΦNE positron ring. When possible simulation results are compared to experimental observations. Conclusions follow in the last section.

II. ELECTRON CLOUD BUILD UP

Photoemission and/or ionization of the residual gas in the beam pipe produces electrons, which move under the action of the beam field, their own space charge, and any magnetic field . These primary electrons are accelerated by the beam, gain energy, and strike the chamber again, producing more electrons. The secondary electron yield, the number of emitted electrons per impinging electron, (SEY) of typical vacuum chamber materials can be ¿1 even after surfacetreatment, leading to an amplification of the cascade. This amplification is counterbalanced by the action of the own space charge of the electrons, and a saturation is reached. A number of sophisticated computer simulation codes, (e.g., PEI[8], POSINST[9],

and ECLOUD [10]), have been developed to study the e-cloud effect, and their predictions have been compared with experimental observations. To study the build up of the electron cloud in the DAΦNE positron ring the code ECLOUD has been used. The input parameters for ECLOUD are collected in Table III. The reflectivity and photo-emission yield values have been obtained by measurements performed on Al samples with the same finishing of the actual vacuum chamber [11]. The secondary emission yield (SEY) curve model used is the one described in [12] scaled to an elastic reflection probability at zero electron energy of 0.5 [13], and with a maximum value $\delta_{max} = 1.9$ as were found for technical Al surfaces after electron conditioning.

TABLE I. DAΦNE beam and pipe parameters used as input for ECLOUD simulations.

parameter	**unit**	**value**
bunch population N_b	10^{10}	2.1
number of bunches N	–	100
missing bunches N_{gap}	–	20
bunch spacing L_{sep}	m	0.8
bunch length σ_z	mm	18
bunch horiz. size σ_x	mm	1.4
bunch vert. size σ_y	mm	0.05
wiggler chamber horiz. aperture $2h_x$	mm	120
wiggler chamber vert. aperture $2h_y$	mm	20
straight sections radius	mm	44
primary photo-emission yield $d\lambda/ds$	–	0.0088
photon reflectivity	–	50%
maximum *SEY* δ_{max}	–	1.9
energy for max. *SEY* E_{max}	eV	250

A. Build Up in the DAΦNE Wigglers

The wiggler magnetic field characterization was performed measuring the vertical magnetic field component By, over a rectangular point matrix on the x-z plane [6]. Starting form

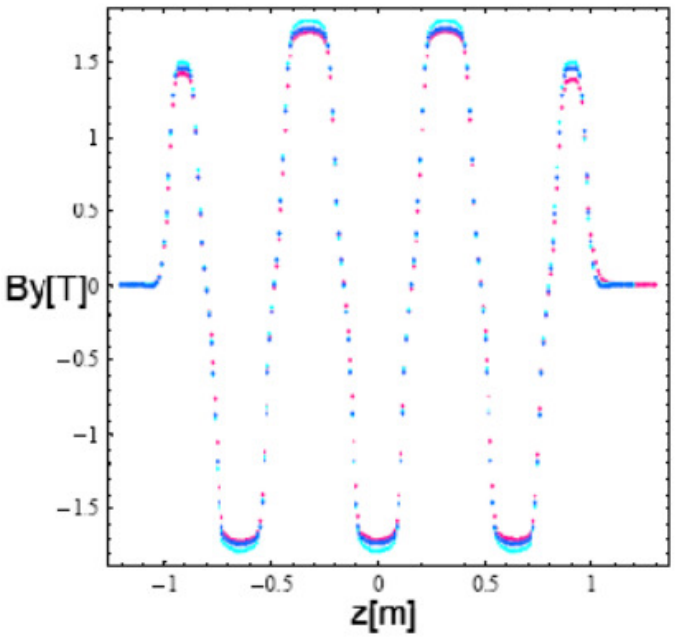

FIG. 1. Vetical component of the magnetic field along the longitudinal axis for the old (blue), current (red), and recently proposed (cyan) wiggler.

these values a spline fit was performed, and the obtainedcoefficients were used for the field reconstruction as showed in [3]. This method has been applied to build three models of the wiggler field, the first corresponding to the wiggler before the pole modification in 2003, the second corresponding to the field after the pole modification (currently installed at DAΦNE), and the third corresponding to a further modification of the wiggler recently proposed to improve field quality and reduce nonlinearities [7].In Figure 1 the field reconstruction results are reported for the three different models.

Using these models of the DAΦNE wiggler field, the electron build-up was simulated. It has to be noted that the presence of the slots has been taken into account considering only the photon flux that is not intercepted by the antechamber (5%). With this prescription part of the electrons are emitted at the position of the antechamber slots. However, since in a dipole magnetic field these electrons contribute little to the multipacting and the electron build up, this approximation does not introduce any noticeable error.

In Figure 2 the electron cloud linear density evolution is reported for the three wiggler magnetic field models discussed above, showing a negligible dependence of the build up on

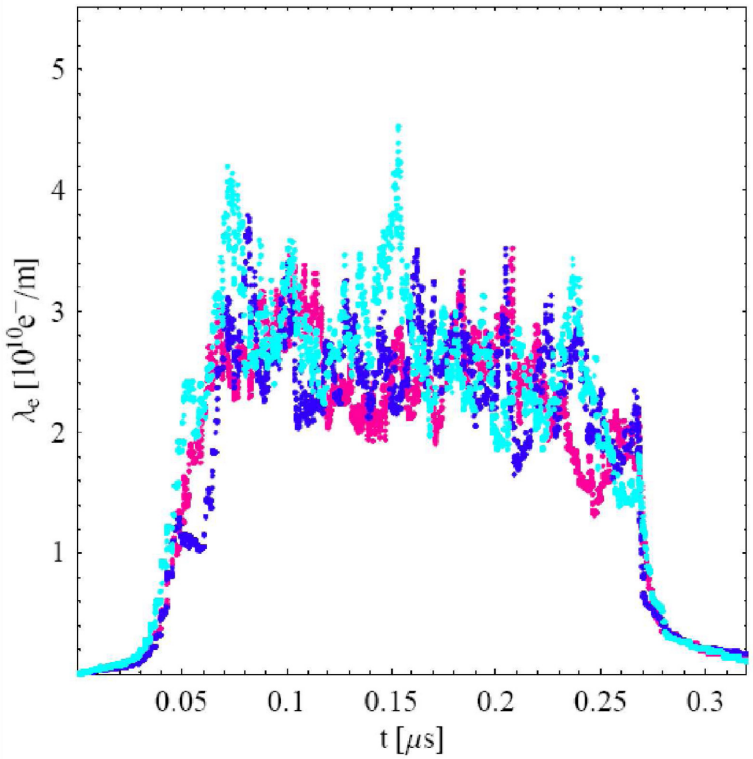

FIG. 2. Electron cloud build up along a DAFNE bunch train for the old (blue),current (red), and recently proposed (cyan) wiggler.

the magnetic field model.

B. Build Up in Solenoidal Field

At the startup after the recent shutdown for the setup of the crab waist collision scheme [13] the instability threshold dropped to $I_{th.} = 270$ mA for the positron current, with the vertical feedback switched off. In the attempt to find a remedy solenoids were installed in the field free regions of DAΦNE, leading to an increase of the threshold to $I_{th.} = 400$ mA. Simulations followed to better understand this mechanism. Here we focus our attention on the electrons accumulated through the secondary emission from the beam pipe in the straight sections. In the simulation, we generate a large number of electrons only at the first bunch passage and let electron cloud develops by the secondary emission process. The electron cloud density build up along the train is shown in Figure 3, for different values of the solenoidal field B_z.

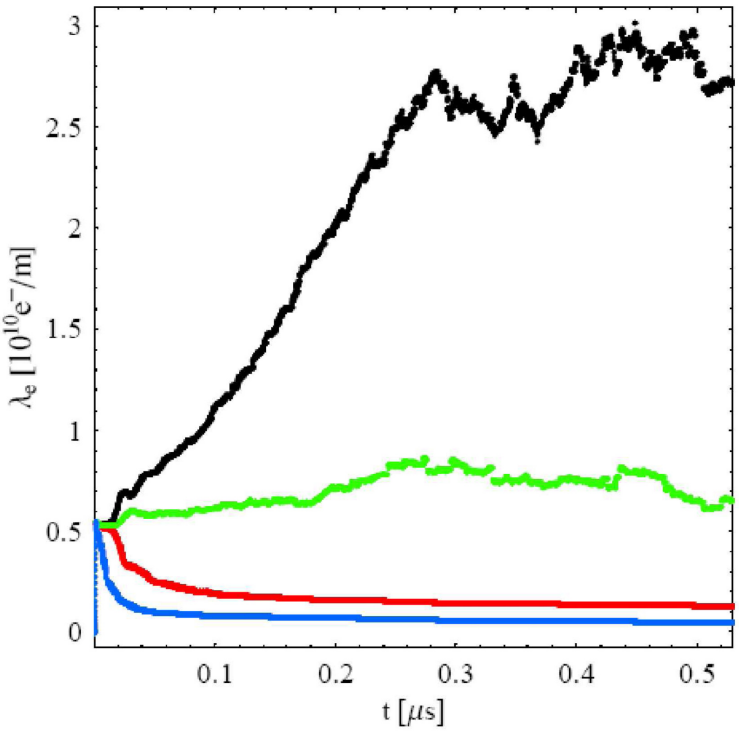

FIG. 3. Density of electron cloud as a function of time for different solenoid settings: $B_z = 0$ G (black), $B_z = 20$ G (green), $B_z = 40$ G (red), $B_z = 60$ G (blue).

Without solenoids (black curve in Figure 3) the average density grows along the train and saturates due to the balance between the space charge and secondary yield. For $B_s > 20$ G electron density decrease very quickly after the passage of the first bunch. A resonance is expected when the time between two consecutive collisions of the electrons in the cloud with the beam pipe surface, that is about half of the electrons cyclotron period T_c, is equal to the time interval between two bunch passage. For the DAΦNE parameters, this condition reads to the following resonance condition for the magnetic field:

$$B_z^c = \frac{\pi m_e c^2}{e L_{sep}} \approx 66 \text{ G}. \tag{1}$$

However there is a threshold value of bunch population, related to the energy gain of the electrons in the cloud during the passage of a bunch and independent of the bunch spacing, above which the resonance takes place. As shown in Figure 4, simulations for DAΦNE exhibit a threshold $N_b = 5 \cdot 10^{10}$ for both single and double bunch spacing that is above the currently operated current. The effectiveness of solenoids in reducing the electron cloud density has also been checked by monitoring the vacuum behaviour for the positron beam.

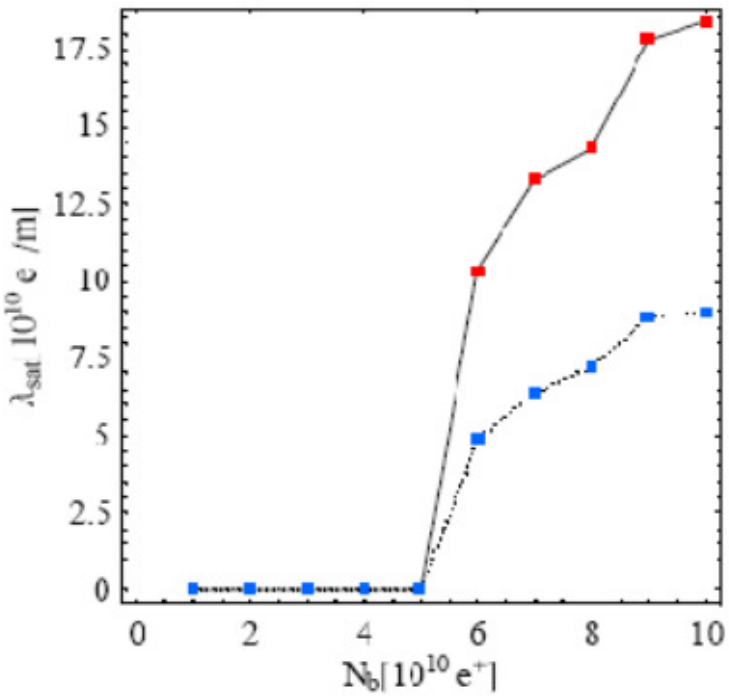

FIG. 4. Saturated density as a function of the bunch population. Red dots represent the case of Lsep spacing and 66G field. Blue dots represent 2Lsep spacing and 33G field.

The vacuum pressure read-out is reported in Figure 5 for the solenoid ON-OFF cases as recorded by a vacuum gauge located in a region of the positron ring where solenois are installed. The pressure reduction in the region with solenoids is clear.

III. ELECTRON CLOUD INDUCED INSTABILITIES

Once the electron cloud is formed, the beam passing through the cloud interacts with it. The motions of bunches become correlated with each other if the memory of a previous bunch is retained in the electron cloud i.e., a small displacement of a bunch creates a perturbation of the electron cloud, which affects the motions of the following bunches, with the result that a coupled-bunch instability is caused. A complete discussion of the electron cloud induced multi-bunch instability formalism is outside the aim of this paper . The reader is referred to [10] for a detailed presentation of the subject. Experimental observations [1-5] show that the horizontal instability affecting the DAΦNE positron beam is a multi-bunch instability. The

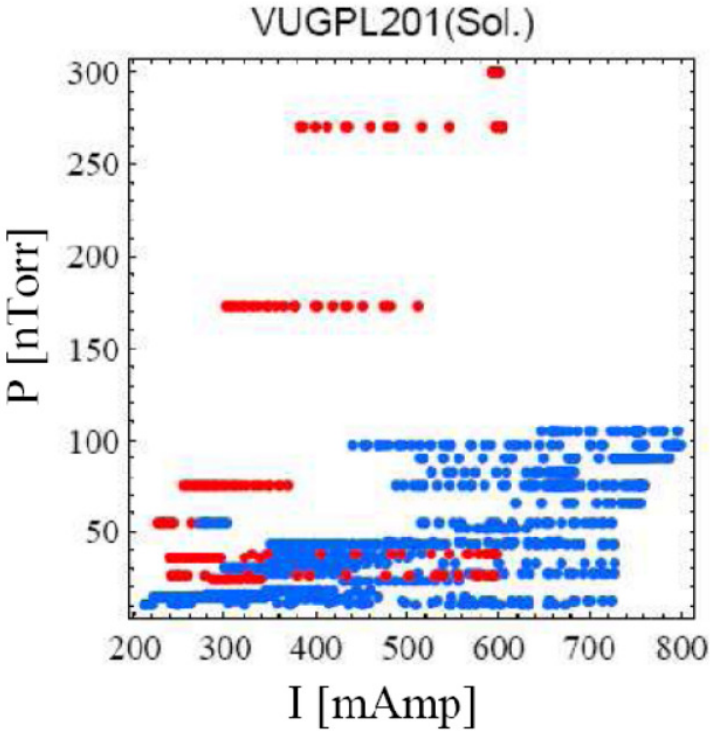

FIG. 5. Vacuum pressure read-out vs. total current as recorded in a straight section of the positron ring where a 40 G solenoidal field was turned on (blue dots) and off (red dots)

observed oscillation mode of the instability is always a very slow frequency mode and can be identified as the -1 mode (i.e., the mode that has a line closest to the frequency origin (zero frequency) from the negative part of the spectrum). The same behaviour has been observed even after the solenoid installation. For this reasons the attention has been focused on the interaction of the beam with the cloud in wigglers and bending magnets where the solenoids are not effective.

A. Tracking of the Coupled-Bunch Instability

A positron bunch can be characterized by its transverse and longitudinal position (dipole moment) as a function of s, ignoring the internal structure of the bunch. Interactions between bunches and electrons in a cloud are determined by the transverse and longitudinal profiles of the bunches. The profiles are assumed to be Gaussian with standard deviation

determined by the emittance and the average beta function in the transverse and longitudinal directions. The motion of each bunch is determined by the transformation representing lattice magnets and the interactions with electrons, while the motions of the electrons are determined by the interactions with the bunches, space charge forces between the electrons, and any magnetic field. The equations of motion are written as

$$\frac{d^2\mathbf{x}^p}{ds^2} + K(s)\mathbf{x}^p = \frac{r_e}{\gamma}\sum_{e=1}^{N}\mathbf{F}(\mathbf{x}^p - \mathbf{x}^e)\delta(s - s^e) \tag{2}$$

$$\frac{d^2\mathbf{x}^e}{dt^2} = 2r_e c^2 \sum_{p=1}^{N_p}\mathbf{F}(\mathbf{x}^e - \mathbf{x}^p)\delta[t - t^p(s^e)] = \frac{e}{m_e}\frac{d\mathbf{x}^e}{dt} \times \mathbf{B} - 2r_e c^2 \frac{\partial \Phi}{\partial \mathbf{x}} \tag{3}$$

where subscripts p and e of $\mathbf{x}$ denote positron and electron, respectively, re is the classical electron radius, me is the electron mass, c is the speed of light, e is the electron charge, Φ is the electric potential due to electrons, δ is the periodic delta function for the circumference, and $\mathbf{F}$ is the Coulomb force in two-dimensional space given by the Bassetti-Erskine formula [11]. To estimate the multi-bunch instability induced by the electron cloud in the arcs of

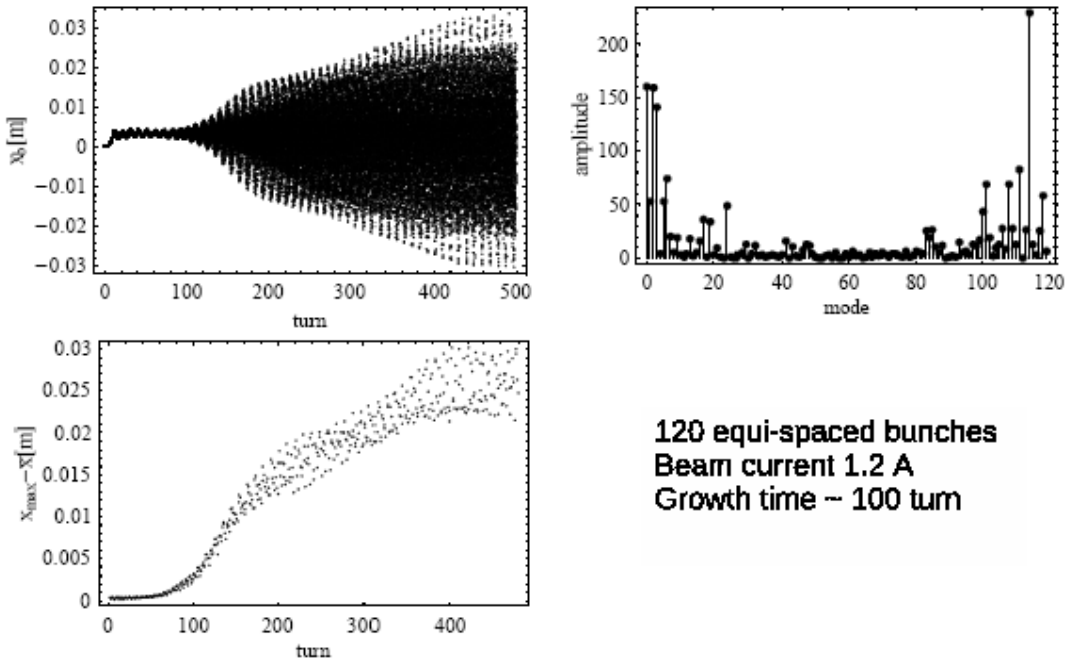

FIG. 6. Beam signal (a), beam envelope (b), and mode spectrum (c) for a completely filled DAFNE bunch train.

the DAΦNE positron ring the code PEI-M [10] has been used. The code computes the

transverse amplitude of each bunch as a function of time by solving equations (2), and (3), while evolving the build-up of the electron cloud self-consistently. To save computation time, the Poisson equation for the space charge potential Φ is solved only once for zero beam amplitude, and is used as a constant field in tracking simulation. The beam and chamber parameters used in the simulation are collected in Table III. A uniform vertical magnetic field $B_z = 1.7$ T was used to model the motion of the electrons both in wigglers and dipoles, and a circular chamber of radius $R = 45$ mm is used instead of the real chamber geometry in order to solve analytically the Poisson equation for Φ. The instability mode spectrum is obtained by taking the Fourier transform of the transverse amplitude of each single bunch as computed by the code, and the grow-rate is obtained by an exponential fit to the beam signal envelope. In Figure 6 are reported the beam signal (the horizontal position of each bunch as a function of time expressed in turns), the beam signal envelope, and the mode spectrum obtained for a bunch train of 120 equi-spaced bunches filled with a beam current of 1.2 A. It is clearly seen that the most unstable mode, obtained by the simulation is mode 114, corresponding to the -1 mode. Experiments on coupled-bunch instabilities have been extensively performed using the DAΦNE fast feedback system to perform grow-dump measurements [2],[4]. Measured grow-rate are compared to simulation results in Table II for different beam currents, showing a good agreement.

TABLE II. Measured and simulated instability growth rate for different beam current.

Measurement		Simulation	
$I[mA]/nb$	τ/T_0	$I[mA]/nb$	τ/T_0
1000/105	73	1200/120	100
750/105	56	900/120	95
500/105	100	600/120	130

B. Simulations of the Single-Bunch Instability

To study the coupled motion of a positron bunch and the electron cloud we used the code CMAD (M.P. SLAC) [8]. The code accepts in input the files sectormap and optics previously generated by running MAD (mad8 or madx) with the ring attice. Sectormap and

optics files respectively include the information on the first and second order transfer maps and the twiss lattice parameters for each element of the ring. The beam is then tracked along the ring by first order R and second order T transfer maps. Typically, the interaction between the beam and the electron cloud is simulated at every element of the ring. The bunch and the cloud are modeled by macroparticles and allowed to move in 3 dimensions (3D). During the beam-cloud interaction, the 2D forces from the beam and the cloud are computed. The bunch is typically sliced longitudinally and a number of kicks are applied to the electron cloud which is pinched by the positive beam potential. The electron cloud space charge force is computed at each bunch slice. The cloud experiences both the electric fields from the beam and the cloud. The dynamics of the electron is computed including the magnetic fields of the element and their position is updated with a Leap-frog and Boris rotation integrator scheme. Finally, the code makes use of parallel simulations to reduce the computation time when dealing with a large number of ring elements. The input

TABLE III. DAΦNE beam parameters used as input for CMAD simulations.

Parameter	Unit	Value
Beam energy E	GeV	0.51
circumference L	m	97.58
bunch population Nb	-	$2.1 \cdot 10^{10}$
bunch length σ_z	um	12
hor. emittance σ_x	um	0.56
vert. emittance σ_y	pm	0.035
hor./vert. bet. tune Qx/Qy	-	5.1/5.2
synchrotron tune Qz	-	0.012
momentum compaction α	-	0.019

parameters for CMAD are collected in Table 1, and in Figure 7 are reported the DAΦNE beta functions, used in the simulation, as obtained by a MADX model that matches quite well beam measurements [9]. To take into account the suppression of the cloud in the drift regions of DAΦNE, where solenoids are installed, the interaction between the bunch and the cloud is computed only in the bending and wiggler sections of the ring. Figure 8 shows emittance growth due to the fast single-bunch instability caused by the electron cloud effect

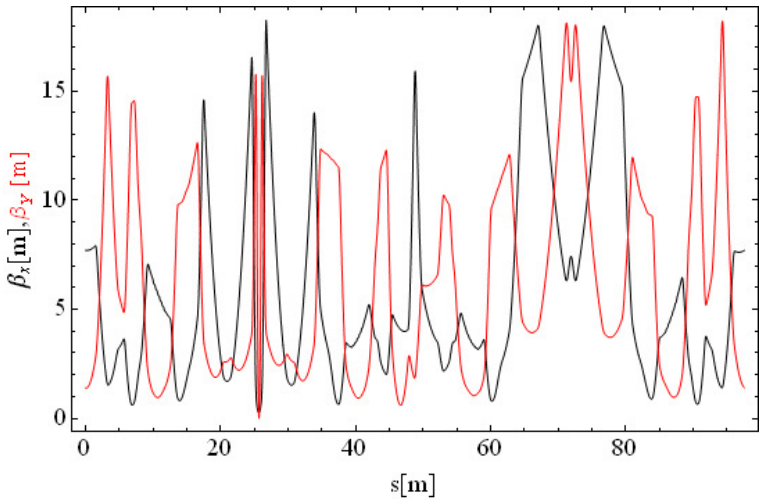

FIG. 7. Horizontal (black) and vertical (red) beta functions as obtained by an accurate MADX model of the DAFNE e+ ring.

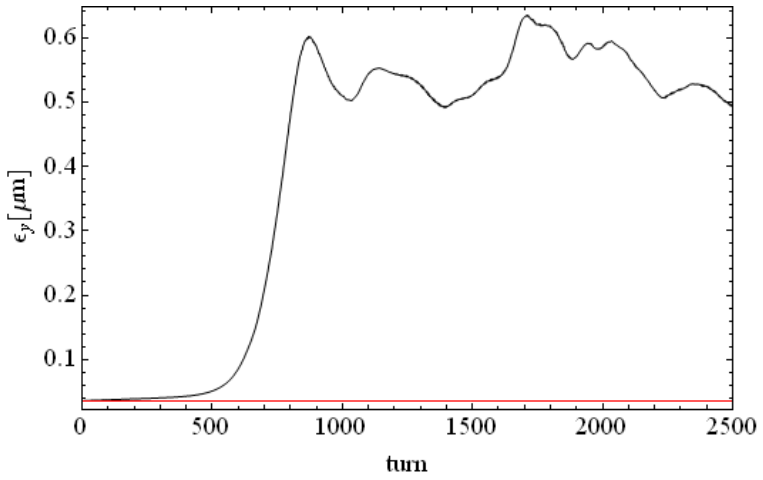

FIG. 8. Vertical emittance growth due to single-bunch instability. The interaction between the beam and the cloud is evaluated in bending and wiggler sections of the DAFNE e+ ring for an electron density $\rho_e = 2 \cdot 10^{13}\mathrm{m}^{-3}$(red) and $\rho_e = 5 \cdot 10^{13}\mathrm{m}^{-3}$ (black).

in the DAΦNE e+ ring. Each line shows an emittance growth for various cloud densities. The threshold density is determined by the density at which the growth starts. From this numerical simulation, we determine that the instability starts at a value of the electron density that is between $\rho_e = 2$ and $5 \cdot 10^{13}$ m^{-3}. This threshold is well above the simulated e-cloud density in wigglers and bending magnets [6].

IV. ELECTRODES DESIGN AND INSTALLATION

To mitigate such instability metallic (copper) electrodes have been inserted in all dipole and wiggler chambers of the machine and have been connected to external dc voltage generators in order to absorb the photo-electrons. Simulations of the e- cloud density and instability threshold with and without the voltage applied to the electrodes are widely discussed in [4]. With a dc voltage of 500 V applied to each electrode we expect a reduction of such density. The pictures of the electrodes inserted in the dipole and wiggler chambers are shown in Figure 9. The dipole electrodes have a length of 1.4 or 1.6 m depending on the considered arc, while the wiggler ones are 1.4 m long. They have a width of 50 mm, thickness of 1.5 mm and their distance from the chamber is about 0.5 mm. This distance is guaranteed by special ceramic supports made in SHAPAL and distributed along the electrodes. This ceramic material is also thermo-conducting in order to partially dissipate the power released from the beam to the electrode through the vacuum chamber (see last paragraph). Moreover, the supports have been designed to minimize their beam coupling impedance and to simultaneously sustain the strip. The mechanical drawing of a dipole-wiggler arc with the electrodes is shown in Figure 10. The distance of the electrode from the beam axis is 8 mm in the wigglers and 25 mm in the dipoles. The electrodes have been connected to the external dc voltage generators modifying the existing BPM flanges as shown in Figure 9. The electrodes have been inserted in the vacuum chamber in the last January-May 2010 shutdown. The electrodes have been inserted in the machine through special plastic supports that allowed inserting the electrodes in the chamber without damaging the chamber and the electrodes themselves. Before and after their installation the electrodes have been tested applying a dc voltage of about 400 V (in air) to check the correct installation and the correct connection of the devices. Measurements with a Network Analyzer have been also done and they will be illustrated in the next section.

V. CONCLUSIONS

Simulations for the DAΦNE wiggler show a negligible dependence of the build up on the magnetic field model, and a build-up variation with bunch filling pattern that is compatible with experimental observations. Simulations for the build up in solenoidal field show that

FIG. 9. Pictures of the electrodes inserted in the dipole (rigth) and wiggler (center) chambers. Detail of the electrodes output connection (left).

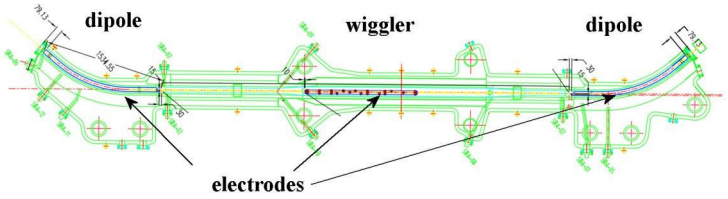

FIG. 10. Mechanical drawing of a complete arc with the electrodes.

a small field is effective in reducing the electron cloud density in straight section, and that the threshold for the cyclotron resonance is above the bunch population currently available in DAΦNE. Also in this case there is a qualitative agreement with observations. Coupled-bunch instability simulations are in good agreement with the experimental observations, and indicate that the observed horizontal instability is compatible with a coupled bunch instability induced by the presence of an electron cloud in the arcs of the DAΦNE positron rings. Work is in progress to include more realistic models for the space charge potential

and the chamber boundaries in the simulation code.

---

[1] C. Vaccarezza, et al, ECLOUD04, Napa Valley proc.

[2] A.Drago et al., Proceedings of PAC09, TH5RFP057.

[3] A.Drago et al., Proceedings of PAC05, p.1841.

[4] C.Vaccarezza et al., Proceedings of PAC05, p.779.

[5] A.Drago, proc. of the 40th ICFA Workshop on High Luminosity e+e- Factories.

[6] A.Drago et al., DAFNE Tech. Notes, G-67.

[7] A.Drago et al., Proceedings of PAC09, TH6REP0762.

[8] T.Demma et al., Proceedings of EPAC08, p.1607.

[9] T.Demma, ICFA Beam Dynamics Newsletter n.48 (2009), pp.64-71.

[10] S.S.Win et al., Phys. Rev. ST Accel. Beams 8, 094401 (2005).

[11] M. Bassetti and G. Erskine, CERN Technical Report No. ISR TH/80-06, 1980.

[12] K. Ohmi, Phys. Rev. Lett. 75, 1526 (1995).

[13] Y.Cai et al., Phys. Rev. ST-AB 7, 024402 (2004).